

A quadratic finite element for the relaxed micromorphic model

Adam Sky^{1,*}, Ingo Muench¹, and Patrizio Neff²

¹ Institute of Structural Mechanics, Statics and Dynamics, TU-Dortmund

² Chair for Nonlinear Analysis and Modelling, Faculty of Mathematics, University Duisburg-Essen

In this work we discuss the relaxed micromorphic model and implementation details for a full three-dimensional formulation entailing a quadratic Lagrangian-Nédélec finite element and appropriate boundary conditions in the discrete setting.

The relaxed micromorphic model is a generalized continuum theory with the capacity to capture more complex kinematical behaviour than in the classical Cauchy continua. Such behaviour is commonly found in materials with a pronounced micro-structure such as porous media and metamaterials. The theory introduces the microdistortion field, encompassing nine additional degrees of freedom for each material point in the continuum, effectively turning each material point into a deformable micro-body. The uncommon discrete formulation stems from the employment of the Curl operator in the energy functional of the relaxed micromorphic model, thus requiring $H(\text{curl})$ -conforming finite elements for well-posedness to be inherited in the discrete setting. The model further introduces the so called consistent coupling condition, which requires some technical considerations in order to be upheld correctly.

This work demonstrates the finite element formulation, culminating with a numerical example.

© 2023 The Authors. *Proceedings in Applied Mathematics & Mechanics* published by Wiley-VCH GmbH.

1 The relaxed micromorphic model

The relaxed micromorphic model [5] is defined by the two-field minimization problem

$$I(\mathbf{u}, \mathbf{P}) = \frac{1}{2} \int_{\Omega} \langle \mathbb{C}_e \text{sym}(\mathbf{D}\mathbf{u} - \mathbf{P}), \text{sym}(\mathbf{D}\mathbf{u} - \mathbf{P}) \rangle + \langle \mathbb{C}_{\text{micro}} \text{sym} \mathbf{P}, \text{sym} \mathbf{P} \rangle + \langle \mathbb{C}_c \text{skew}(\mathbf{D}\mathbf{u} - \mathbf{P}), \text{skew}(\mathbf{D}\mathbf{u} - \mathbf{P}) \rangle + \mu_{\text{macro}} L_c^2 \|\text{Curl} \mathbf{P}\|^2 dX - \int_{\Omega} \langle \mathbf{u}, \mathbf{f} \rangle + \langle \mathbf{P}, \mathbf{M} \rangle dX \rightarrow \min \text{ w.r.t. } \{\mathbf{u}, \mathbf{P}\}, \quad (1)$$

where $\mathbf{u} : \Omega \subset \mathbb{R}^3 \rightarrow \mathbb{R}^3$ and $\mathbf{P} : \Omega \subset \mathbb{R}^3 \rightarrow \mathbb{R}^{3 \times 3}$ are the displacement and the microdistortion fields, respectively. The tensors \mathbb{C}_e and $\mathbb{C}_{\text{micro}}$ are standard fourth order elasticity tensors and \mathbb{C}_c is a positive semi-definite coupling tensor for infinitesimal rotations. The macroscopic shear modulus is denoted by μ_{macro} and the parameter $L_c \geq 0$ represents the characteristic length scale motivated by the geometry of the microstructure. The body forces and micro-moments are given by \mathbf{f} and \mathbf{M} , respectively. The differential operators are defined as

$$\mathbf{D}\mathbf{u} = \begin{bmatrix} u_{1,1} & u_{1,2} & u_{1,3} \\ u_{2,1} & u_{2,2} & u_{2,3} \\ u_{3,1} & u_{3,2} & u_{3,3} \end{bmatrix}, \quad \text{Curl} \mathbf{P} = \begin{bmatrix} \text{curl} [P_{11} & P_{12} & P_{13}] \\ \text{curl} [P_{21} & P_{22} & P_{23}] \\ \text{curl} [P_{31} & P_{32} & P_{33}] \end{bmatrix}, \quad \text{curl} \mathbf{p} = \nabla \times \mathbf{p}. \quad (2)$$

In this work we consider isotropic materials, such that the material tensors read

$$\mathbb{C}_e = 2\mu_e \mathbb{J} + \lambda_e \mathbb{1} \otimes \mathbb{1}, \quad \mathbb{C}_{\text{micro}} = 2\mu_{\text{micro}} \mathbb{J} + \lambda_{\text{micro}} \mathbb{1} \otimes \mathbb{1}, \quad \mathbb{C}_c = 2\mu_c \mathbb{A}, \quad (3)$$

where $\mathbb{J} : \mathbb{R}^{3 \times 3} \mapsto \mathbb{R}^{3 \times 3}$ and $\mathbb{A} : \mathbb{R}^{3 \times 3} \mapsto \mathfrak{so}(3)$ are the fourth order identity and anti-symmetry tensors, respectively. Variations with respect to the displacement and the microdistortion fields $\{\mathbf{u}, \mathbf{P}\}$ lead to the bilinear and linear forms

$$a(\{\delta \mathbf{u}, \delta \mathbf{P}\}, \{\mathbf{u}, \mathbf{P}\}) = \int_{\Omega} \langle \mathbb{C}_e \text{sym}(\mathbf{D}\delta \mathbf{u} - \delta \mathbf{P}), \text{sym}(\mathbf{D}\mathbf{u} - \mathbf{P}) \rangle + \langle \mathbb{C}_{\text{micro}} \text{sym} \delta \mathbf{P}, \text{sym} \mathbf{P} \rangle + \langle \mathbb{C}_c \text{skew}(\mathbf{D}\delta \mathbf{u} - \delta \mathbf{P}), \text{skew}(\mathbf{D}\mathbf{u} - \mathbf{P}) \rangle + \mu_{\text{macro}} L_c^2 \langle \text{Curl} \delta \mathbf{P}, \text{Curl} \mathbf{P} \rangle dX, \quad (4a)$$

$$l(\{\delta \mathbf{u}, \delta \mathbf{P}\}) = \int_{\Omega} \langle \delta \mathbf{u}, \mathbf{f} \rangle + \langle \delta \mathbf{P}, \mathbf{M} \rangle dX. \quad (4b)$$

* Corresponding author: e-mail: adam.sky@tu-dortmund.de



This is an open access article under the terms of the Creative Commons Attribution-NonCommercial-NoDerivs License, which permits use and distribution in any medium, provided the original work is properly cited, the use is non-commercial and no modifications or adaptations are made.

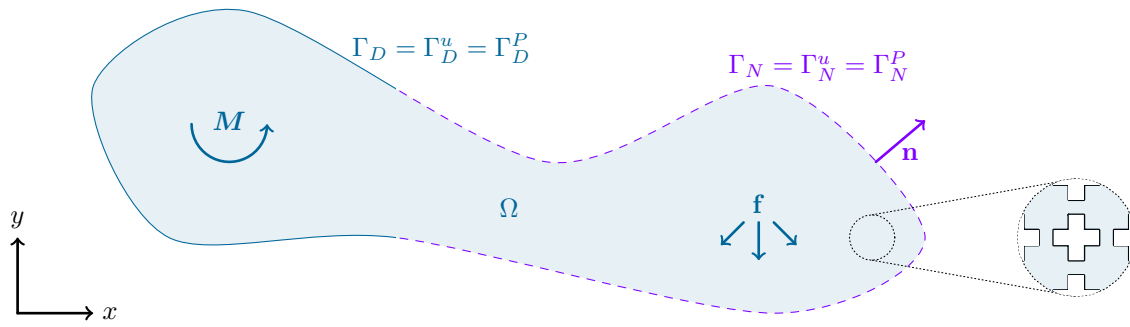


Fig. 1: A micro-structured domain in the relaxed micromorphic model with Dirichlet and Neumann boundaries under internal forces and micro-moments. The Dirichlet boundary of the microdistortion is given by the consistent coupling condition.

By partial integration and splitting of the boundary between Dirichlet and Neumann boundaries, one finds the strong form

$$-\text{Div}[\mathbb{C}_e \text{sym}(\mathbf{D}\mathbf{u} - \mathbf{P}) + \mathbb{C}_c \text{skew}(\mathbf{D}\mathbf{u} - \mathbf{P})] = \mathbf{f} \quad \text{in } \Omega, \quad (5a)$$

$$-\mathbb{C}_e \text{sym}(\mathbf{D}\mathbf{u} - \mathbf{P}) - \mathbb{C}_c \text{skew}(\mathbf{D}\mathbf{u} - \mathbf{P}) + \mathbb{C}_{\text{micro}} \text{sym} \mathbf{P} + \mu_{\text{macro}} L_c^2 \text{Curl}(\text{Curl} \mathbf{P}) = \mathbf{M} \quad \text{in } \Omega, \quad (5b)$$

$$\mathbf{u} = \tilde{\mathbf{u}} \quad \text{on } \Gamma_D^u, \quad (5c)$$

$$\mathbf{P} \times \mathbf{n} = \tilde{\mathbf{P}} \times \mathbf{n} \quad \text{on } \Gamma_D^P, \quad (5d)$$

$$[\mathbb{C}_e \text{sym}(\mathbf{D}\mathbf{u} - \mathbf{P}) + \mathbb{C}_c \text{skew}(\mathbf{D}\mathbf{u} - \mathbf{P})] \mathbf{n} = 0 \quad \text{on } \Gamma_N^u, \quad (5e)$$

$$\text{Curl} \mathbf{P} \times \mathbf{n} = 0 \quad \text{on } \Gamma_N^P, \quad (5f)$$

where \mathbf{n} denotes the outer unit normal vector, such that $\mathbf{P} \times \mathbf{n}$ is the projection to the tangent surface on the boundary. The terms $\tilde{\mathbf{u}}$ and $\tilde{\mathbf{P}}$ are the prescribed displacement and microdistortion fields on Γ_D^u and Γ_D^P , respectively, see Fig. 1. For the Dirichlet boundary, the relaxed micromorphic theory introduces the so called consistent coupling condition [2]

$$\mathbf{P} \times \mathbf{n} = \mathbf{D}\tilde{\mathbf{u}} \times \mathbf{n} \quad \text{on } \Gamma_D^P, \quad (6)$$

where the prescribed displacement $\tilde{\mathbf{u}}$ on the boundary automatically prescribes the tangential component of the microdistortion \mathbf{P} on the same boundary, effectively inducing the definitions $\Gamma_D = \Gamma_D^P = \Gamma_D^u$ and $\Gamma_N = \Gamma_N^P = \Gamma_N^u$.

1.1 Lower limit of the characteristic length scale parameter $L_c \rightarrow 0$

In the relaxed micromorphic model the characteristic length parameter L_c controls the influence of the underlying micro-structure. In the lower limit $L_c \rightarrow 0$ the continuum is fully homogeneous [1, 4] and Eq. (5b) reduces to

$$-\mathbb{C}_e \text{sym}(\mathbf{D}\mathbf{u} - \mathbf{P}) - \mathbb{C}_c \text{skew}(\mathbf{D}\mathbf{u} - \mathbf{P}) + \mathbb{C}_{\text{micro}} \text{sym} \mathbf{P} = \mathbf{M}, \quad (7)$$

which is used to express the microdistortion \mathbf{P} algebraically

$$\text{sym} \mathbf{P} = (\mathbb{C}_e + \mathbb{C}_{\text{micro}})^{-1} (\text{sym} \mathbf{M} + \mathbb{C}_e \text{sym} \mathbf{D}\mathbf{u}), \quad \text{skew} \mathbf{P} = \mathbb{C}_c^{-1} \text{skew} \mathbf{M} + \text{skew} \mathbf{D}\mathbf{u}. \quad (8)$$

Setting $\mathbf{M} = 0$ corresponds to Cauchy continua where micro-moments do not occur, such that

$$\mathbb{C}_c \text{skew}(\mathbf{D}\mathbf{u} - \mathbf{P}) = 0, \quad \mathbb{C}_e \text{sym}(\mathbf{D}\mathbf{u} - \mathbf{P}) = \mathbb{C}_{\text{micro}} \text{sym} \mathbf{P}, \quad \text{sym} \mathbf{P} = (\mathbb{C}_e + \mathbb{C}_{\text{micro}})^{-1} \mathbb{C}_e \text{sym} \mathbf{D}\mathbf{u}. \quad (9)$$

The latter result in conjunction with Eq. (5a) yields

$$-\text{Div}[\mathbb{C}_e \text{sym}(\mathbf{D}\mathbf{u} - \mathbf{P})] = -\text{Div}[\mathbb{C}_{\text{micro}} (\mathbb{C}_e + \mathbb{C}_{\text{micro}})^{-1} \mathbb{C}_e \text{sym} \mathbf{D}\mathbf{u}] = -\text{Div}[\mathbb{C}_{\text{macro}} \text{sym} \mathbf{D}\mathbf{u}] = \mathbf{f}, \quad (10)$$

where the definition $\mathbb{C}_{\text{macro}} = \mathbb{C}_{\text{micro}} (\mathbb{C}_e + \mathbb{C}_{\text{micro}})^{-1} \mathbb{C}_e$ relates the meso- and micro-elasticity tensors to the macro-elasticity tensor of an equivalent Cauchy continuum, which also arises from standard homogenization for large periodic structures [1, 4]. As such, for isotropic materials the parameters are directly derived via

$$\mu_{\text{macro}} = \frac{\mu_e \mu_{\text{micro}}}{\mu_e + \mu_{\text{micro}}}, \quad 2\mu_{\text{macro}} + 3\lambda_{\text{macro}} = \frac{(2\mu_e + 3\lambda_e)(2\mu_{\text{micro}} + 3\lambda_{\text{micro}})}{(2\mu_e + 3\lambda_e) + (2\mu_{\text{micro}} + 3\lambda_{\text{micro}})}. \quad (11)$$

1.2 Upper limit of the characteristic length scale parameter $L_c \rightarrow +\infty$

The case $L_c \rightarrow +\infty$ can be interpreted as the entire domain being the micro-body itself. However, in practice, the limit is given by the size of one unit cell. Since the energy functional is being minimized, on contractible domains this implies the reduction of the microdistortion to a gradient field $\mathbf{P} \rightarrow \text{D}\mathbf{v}$ due to the classical identity $\text{Curl D}\mathbf{v} = 0 \forall \mathbf{v} \in [C^\infty(\Omega)]^3$, thus assuring finite energies for large characteristic length values. Since only the micro-body is considered, one sets $\mathbf{f} = 0$ to find

$$-\text{Div}[\mathbb{C}_e \text{sym}(\text{D}\mathbf{u} - \mathbf{P}) + \mathbb{C}_c \text{skew}(\text{D}\mathbf{u} - \mathbf{P})] = 0, \tag{12}$$

for Eq. (5a). As such, taking the divergence of Eq. (5b) yields

$$\text{Div}(\mathbb{C}_{\text{micro}} \text{sym D}\mathbf{v}) = \text{Div } \mathbf{M}. \tag{13}$$

The divergence of the micro-moments $\text{Div } \mathbf{M}$ can be interpreted as the micro body-forces. Consequently, the limit $L_c \rightarrow +\infty$ defines an equivalent Cauchy continuum with a finite stiffness $\mathbb{C}_{\text{micro}}$, representing the upper limit for the relaxed micromorphic model [1, 4]. Due to Eq. (12) and the consistent coupling condition Eq. (6) there holds $\mathbf{v} = \mathbf{u}$ as the solution is unique.

2 Finite element formulations

The construction of quadratic conforming tetrahedral finite elements $\mathcal{L}^2 \times \mathcal{N}_{II}^1 \subset H^1 \times H(\text{curl})$ with a Lagrangian and Nédélec basis [6, 8, 9] is presented in the following. The elements are mapped from the reference element

$$T = \{\xi, \eta, \zeta \in [0, 1] \mid \xi + \eta + \zeta \leq 1\}, \tag{14}$$

to the physical domain using the barycentric base functions

$$b_1(\xi, \eta, \zeta) = 1 - \xi - \eta - \zeta, \quad b_2(\xi, \eta, \zeta) = \xi, \quad b_3(\xi, \eta, \zeta) = \eta, \quad b_4(\xi, \eta, \zeta) = \zeta, \tag{15}$$

$$\mathbf{x}(\xi, \eta, \zeta) = (1 - \xi - \eta - \zeta) \mathbf{x}_1 + \xi \mathbf{x}_2 + \eta \mathbf{x}_3 + \zeta \mathbf{x}_4, \quad \mathbf{J} = [\mathbf{x}_2 - \mathbf{x}_1 \quad \mathbf{x}_3 - \mathbf{x}_1 \quad \mathbf{x}_4 - \mathbf{x}_1], \tag{16}$$

where \mathbf{x}_i are the vertex coordinates of each tetrahedron on the physical domain and \mathbf{J} is the corresponding Jacobi matrix. The complete domain is given by the union of all elements.

2.1 Lagrangian base functions

The Lagrangian basis has the nodal degrees of freedom

$$l_{ij}(u) = \delta_{ij} u \Big|_{x_j}, \tag{17}$$

where δ_{ij} is the Kronecker delta. Employing the quadratic polynomial space $P^2(T)$, one finds the base functions

$$\begin{aligned} n_1(\xi, \eta, \zeta) &= 2(\eta + \xi + \zeta - 0.5)(\eta + \xi + \zeta - 1), & n_2(\xi, \eta, \zeta) &= 2\xi(\xi - 0.5), \\ n_3(\xi, \eta, \zeta) &= 2\eta(\eta - 0.5), & n_4(\xi, \eta, \zeta) &= 2\zeta(\zeta - 0.5), \\ n_5(\xi, \eta, \zeta) &= 4\xi(1 - \eta - \xi - \zeta), & n_6(\xi, \eta, \zeta) &= 4\eta\xi, \\ n_7(\xi, \eta, \zeta) &= 4\eta(1 - \eta - \xi - \zeta), & n_8(\xi, \eta, \zeta) &= 4\zeta(1 - \eta - \xi - \zeta), \\ n_9(\xi, \eta, \zeta) &= 4\xi\zeta, & n_{10}(\xi, \eta, \zeta) &= 4\eta\zeta, \end{aligned} \tag{18}$$

where n_1 to n_4 are vertex base functions and n_5 to n_{10} are edge base functions defined on the edge midpoint, see Fig. 2.

2.2 Nédélec base functions

The linear Nédélec basis of the second type [3, 8, 10] is defined by the following edge degrees of freedom

$$l_{ij}(\mathbf{p}) = \int_{\mu_i} q_j \langle \mathbf{p}, \boldsymbol{\tau} \rangle d\mu \quad \forall q_j \in P^1(\mu_i), \tag{19}$$

where μ_i is the curve of an edge on the reference element and q_j is a test function. The corresponding polynomial space is $[P^1(T)]^3$, such that 12 base functions define the basis. Using the degrees of freedom for each edge on the reference element

$$\begin{aligned} l_{ij}(\boldsymbol{\vartheta}) &= \int_{\mu_i} q_j \langle \boldsymbol{\vartheta}, \boldsymbol{\varsigma} \rangle d\mu = \delta_{ij}, & q_1(\mu_i) &= 4 - 6\mu_i, & q_2(\mu_i) &= 6\mu_i - 2, & \text{for } \mu_i \in [0, 1], \\ l_{ij}(\boldsymbol{\vartheta}) &= \int_{\mu_i} q_j \langle \boldsymbol{\vartheta}, \boldsymbol{\varsigma} \rangle d\mu = \delta_{ij}, & q_1(\mu_i) &= 2\sqrt{2} - 3\mu_i, & q_2(\mu_i) &= 3\mu_i - \sqrt{2}, & \text{for } \mu_i \in [0, \sqrt{2}], \end{aligned} \tag{20}$$

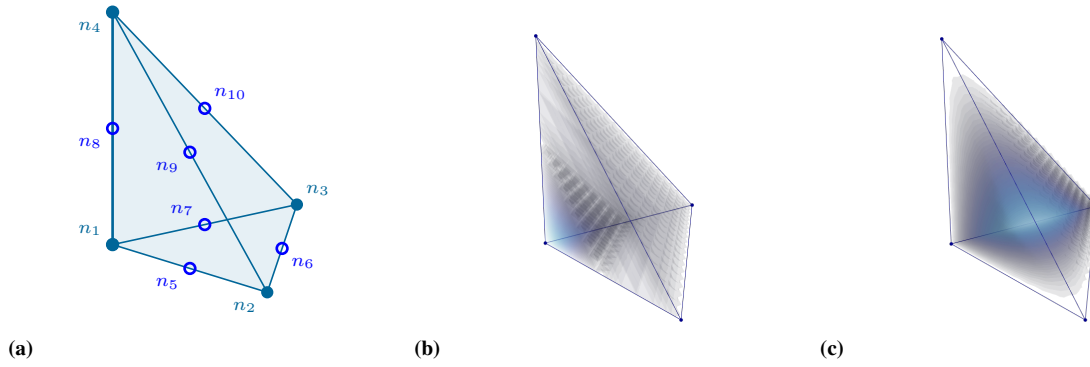


Fig. 2: Vertex and edge nodes on the reference element (a), vertex base function n_1 (b) and edge base function n_7 (c) of the Lagrangian basis.

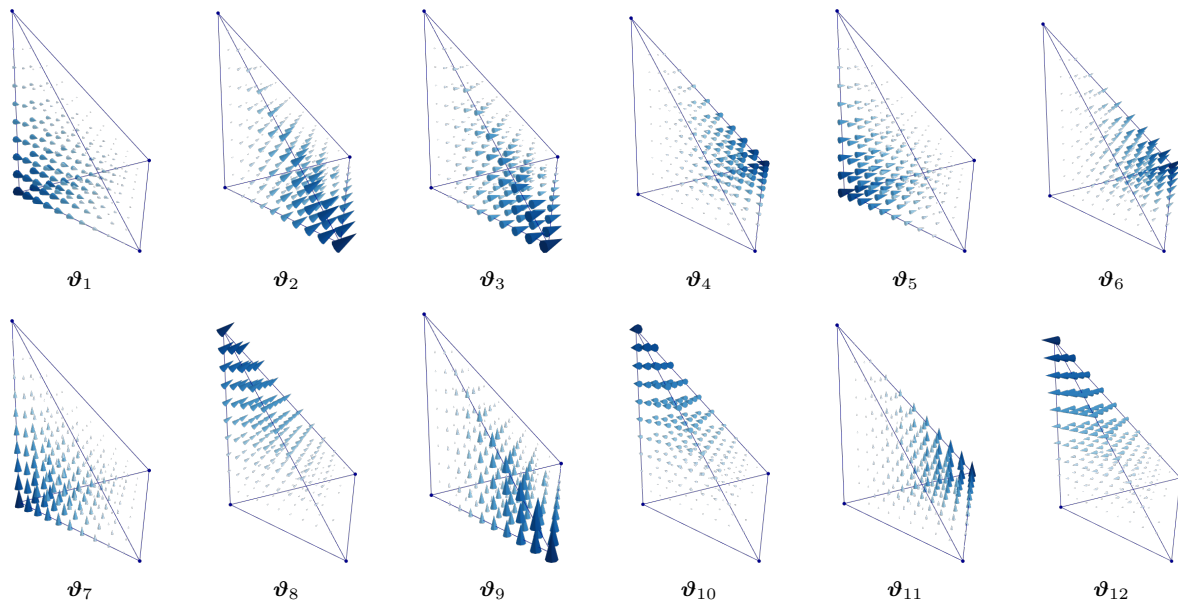


Fig. 3: Nédélec \mathcal{N}^1_{II} -base functions on the reference element.

where μ_i is the parameter for the corresponding edge, we find the following base functions, depicted in Fig. 3

$$\begin{aligned}
 \boldsymbol{\vartheta}_1 &= \begin{bmatrix} 1 - \xi - \eta - \zeta \\ 0 \\ 0 \end{bmatrix}, & \boldsymbol{\vartheta}_2 &= \begin{bmatrix} \xi \\ \xi \\ \xi \end{bmatrix}, & \boldsymbol{\vartheta}_3 &= \begin{bmatrix} 0 \\ \xi \\ 0 \end{bmatrix}, & \boldsymbol{\vartheta}_4 &= \begin{bmatrix} -\eta \\ 0 \\ 0 \end{bmatrix}, \\
 \boldsymbol{\vartheta}_5 &= \begin{bmatrix} 0 \\ 1 - \xi - \eta - \zeta \\ 0 \end{bmatrix}, & \boldsymbol{\vartheta}_6 &= \begin{bmatrix} \eta \\ \eta \\ \eta \end{bmatrix}, & \boldsymbol{\vartheta}_7 &= \begin{bmatrix} 0 \\ 0 \\ 1 - \xi - \eta - \zeta \end{bmatrix}, & \boldsymbol{\vartheta}_8 &= \begin{bmatrix} \zeta \\ \zeta \\ \zeta \end{bmatrix}, \\
 \boldsymbol{\vartheta}_9 &= \begin{bmatrix} 0 \\ 0 \\ \xi \end{bmatrix}, & \boldsymbol{\vartheta}_{10} &= \begin{bmatrix} -\zeta \\ 0 \\ 0 \end{bmatrix}, & \boldsymbol{\vartheta}_{11} &= \begin{bmatrix} 0 \\ 0 \\ \eta \end{bmatrix}, & \boldsymbol{\vartheta}_{12} &= \begin{bmatrix} 0 \\ -\zeta \\ 0 \end{bmatrix}.
 \end{aligned} \tag{21a}$$

The base functions are defined on the reference element. In order to preserve their tangential projection on edges in the physical domain we make use of the covariant Piola transformation [7, 8, 10]

$$\langle \boldsymbol{\theta}, d\mathbf{s} \rangle = \langle \boldsymbol{\theta}, \mathbf{J} d\boldsymbol{\mu} \rangle = \langle \boldsymbol{\vartheta}, d\boldsymbol{\mu} \rangle \iff \boldsymbol{\theta} = \mathbf{J}^{-T} \boldsymbol{\vartheta}. \tag{22}$$

Further, for the curl we find the contravariant Piola transformation [8, 10]

$$\text{curl}_x \boldsymbol{\theta} = \nabla_x \times \boldsymbol{\theta} = (\mathbf{J}^{-T} \nabla_\xi) \times (\mathbf{J}^{-T} \boldsymbol{\vartheta}) = \text{Cof}(\mathbf{J}^{-T}) \text{curl}_\xi \boldsymbol{\vartheta} = \frac{1}{\det \mathbf{J}} \mathbf{J} \text{curl}_\xi \boldsymbol{\vartheta}. \tag{23}$$

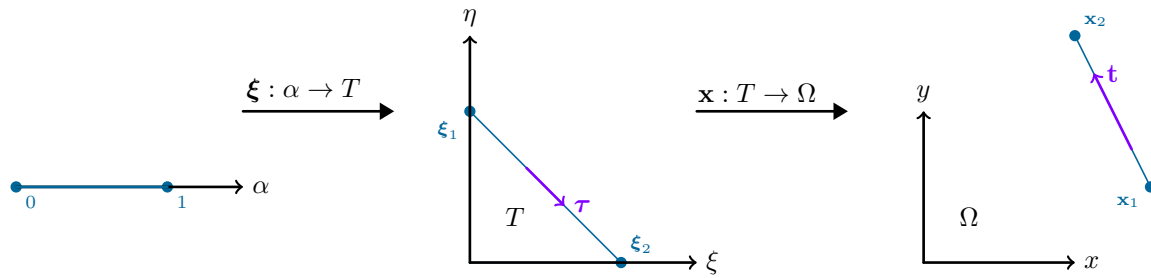


Fig. 4: Barycentric mapping of edges from the unit domain to the reference element and onto the physical domain.

2.3 Boundary conditions

The Dirichlet boundary conditions of the displacement are applied using the point-wise evaluation of the Lagrangian functionals Eq. (17). As such, on each edge of the Dirichlet boundary there exists the following parametrization for $\alpha \in [0, 1]$

$$(\Pi_g u) \circ \alpha \Big|_s = \tilde{u} \Big|_{v_1} n_1(\alpha) + \tilde{u} \Big|_{v_m} n_m(\alpha) + \tilde{u} \Big|_{v_2} n_2(\alpha) = \tilde{u} \Big|_{v_1} (2\alpha - 1)(\alpha - 1) + \tilde{u} \Big|_{v_m} 4\alpha(1 - \alpha) + \tilde{u} \Big|_{v_2} \alpha(2\alpha - 1), \tag{24a}$$

where the vertices v_1 and v_2 represent the start and the end of the edge, and the midpoint of the edge is given by v_m .

In order to satisfy the consistent coupling condition, we first build the Lagrangian interpolation of the displacement field on the Dirichlet boundary and use its gradient to set the boundary condition of the microdistortion. We consider one row of the displacement and the microdistortion fields at a time. Each edge of the finite element mesh is mapped from the unit domain by the barycentric coordinates (see Fig. 4)

$$\mathbf{x}(\alpha) = \lambda_1 \mathbf{x}_1 + \lambda_2 \mathbf{x}_2 = (1 - \alpha)\mathbf{x}_1 + \alpha\mathbf{x}_2, \quad \boldsymbol{\xi}(\alpha) = \lambda_1 \boldsymbol{\xi}_1 + \lambda_2 \boldsymbol{\xi}_2 = (1 - \alpha)\boldsymbol{\xi}_1 + \alpha\boldsymbol{\xi}_2. \tag{25}$$

Consequently, the chain rule allows to simplify the consistent coupling condition to

$$\frac{d}{d\alpha}(u \circ \mathbf{x} \circ \boldsymbol{\xi})(\alpha) = \langle \nabla_{\boldsymbol{\xi}} u, \boldsymbol{\tau} \rangle = \langle \nabla_x u, \mathbf{t} \rangle, \quad \langle \mathbf{p}^h, \mathbf{t} \rangle \Big|_{\Gamma_D} = \frac{d}{d\alpha} \Pi_g \tilde{u} \Big|_{\Gamma_D}. \tag{26}$$

In the quadratic sequence $\mathcal{L}^2 \xrightarrow{\nabla} \mathcal{N}_{II}^1$ on each vertex of an edge, the Nédélec base functions produce a tangential projection of one. As such, the evaluation can be carried out via

$$\begin{aligned} c_1 &= \langle c_1 \boldsymbol{\theta}_1, \mathbf{t} \rangle \Big|_{v_1} = \frac{d}{d\alpha} \left(\tilde{u} \Big|_{v_1} (2\alpha - 1)(\alpha - 1) + \tilde{u} \Big|_{v_m} 4\alpha(1 - \alpha) + \tilde{u} \Big|_{v_2} \alpha(2\alpha - 1) \right) \Big|_{v_1} = -3\tilde{u} \Big|_{v_1} + 4\tilde{u} \Big|_{v_m} - \tilde{u} \Big|_{v_2}, \\ c_2 &= \langle c_2 \boldsymbol{\theta}_2, \mathbf{t} \rangle \Big|_{v_2} = \frac{d}{d\alpha} \left(\tilde{u} \Big|_{v_2} (2\alpha - 1)(\alpha - 1) + \tilde{u} \Big|_{v_m} 4\alpha(1 - \alpha) + \tilde{u} \Big|_{v_1} \alpha(2\alpha - 1) \right) \Big|_{v_2} = \tilde{u} \Big|_{v_1} - 4\tilde{u} \Big|_{v_m} + 3\tilde{u} \Big|_{v_2}, \end{aligned} \tag{27}$$

for each edge s_i in Γ_D . Therefore, the tangential projection of the microdistortion on each edge of Γ_D reads

$$\langle \mathbf{t}, \Pi_c \mathbf{p} \rangle \Big|_{s_i} = \langle \mathbf{t}, c_1 \boldsymbol{\theta}_1 + c_2 \boldsymbol{\theta}_2 \rangle \Big|_{s_i}. \tag{28}$$

3 Numerical example

We demonstrate the influence of the characteristic length scale parameter L_c by measuring the energy for an artificial material with

$$\lambda_{\text{macro}} = 2, \quad \mu_{\text{macro}} = 1, \quad \lambda_{\text{micro}} = 10, \quad \mu_{\text{micro}} = 5, \quad \mu_c = 1, \tag{29}$$

such that the meso-parameters given by Eq. (11) result in

$$\lambda_e = 2.5, \quad \mu_e = 1.25. \tag{30}$$

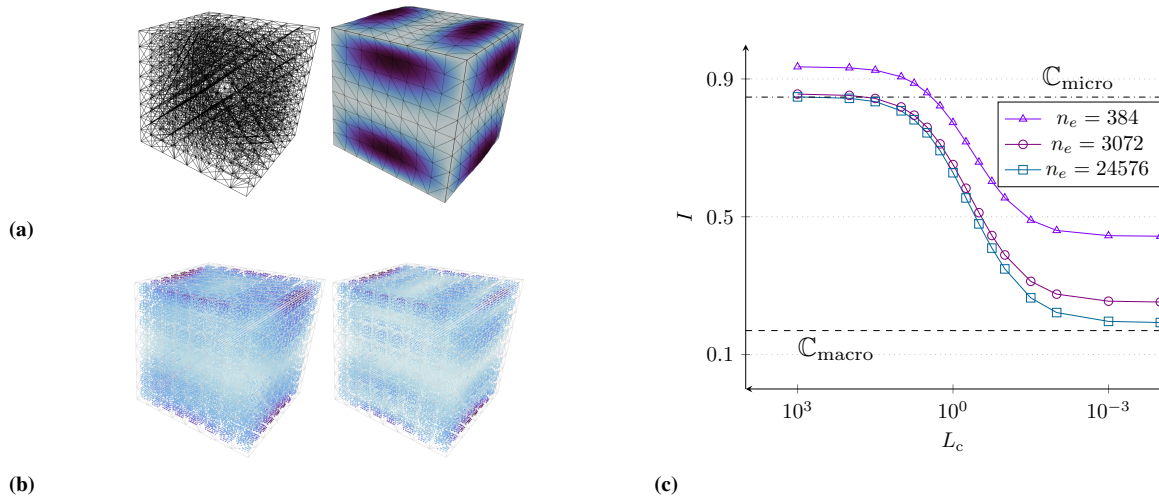


Fig. 5: Mesh with 3072 elements and 39844 degrees of freedom, and displacement field (a). Intensity of the microdistortion for $L_c = 10^2$ and $L_c = 10^{-2}$ (b), respectively. Energy progression of the relaxed micromorphic model with respect to L_c for various discretizations (c).

Further, we employ periodic Dirichlet boundary conditions

$$\begin{aligned} \tilde{u} \Big|_{x=\pm 1} &= \begin{bmatrix} (1-y^2) \sin(\pi[1-z^2])/10 \\ 0 \\ 0 \end{bmatrix}, & \tilde{u} \Big|_{y=\pm 1} &= \begin{bmatrix} 0 \\ (1-x^2) \sin(\pi[1-z^2])/10 \\ 0 \end{bmatrix}, \\ \tilde{u} \Big|_{z=\pm 1} &= \begin{bmatrix} 0 \\ 0 \\ (1-y^2) \sin(\pi[1-x^2])/10 \end{bmatrix}, & & \end{aligned} \quad (31)$$

on the entire boundary $\Gamma_D = \partial\Omega$ of the cubic domain $\bar{\Omega} = [-1, 1]^3$.

The displacement and microdistortion fields are depicted in Fig. 5 (a)-(b). In order to compute the upper and lower bound on the energy we utilize the equivalent Cauchy model formulation with the micro- and macro elasticity parameters. The progression of the energy in dependence of the characteristic length parameter L_c is given in Fig. 5 (e). We clearly observe the ability of the model to iterate between micro- and macro-reactions using the parameter. Further, we note the mesh dependency of the formulation, where the energy is clearly overestimated for coarse meshes. As such, we conclude the necessity of fine meshes for satisfactory approximations.

Acknowledgements Patrizio Neff acknowledges support in the framework of the DFG-Priority Programme 2256 “Variational Methods for Predicting Complex Phenomena in Engineering Structures and Materials”, Neff 902/10-1, Project-No. 440935806. Open access funding enabled and organized by Projekt DEAL.

References

- [1] Aivaliotis, A., Tallarico, D., d’Agostino, M.V., Daouadji, A., Neff, P., Madeo, A.: Frequency- and angle-dependent scattering of a finite-sized meta-structure via the relaxed micromorphic model. *Archive of Applied Mechanics* **90**(5), 1073–1096 (2020)
- [2] d’Agostino, M.V., Rizzi, G., Khan, H., Lewintan, P., Madeo, A., Neff, P.: The consistent coupling boundary condition for the classical micromorphic model: existence, uniqueness and interpretation of parameters. *Continuum Mechanics and Thermodynamics* (2022)
- [3] Nédélec, J.C.: A new family of mixed finite elements in \mathbb{R}^3 . *Numerische Mathematik* **50**(1), 57–81 (1986)
- [4] Neff, P., Eidel, B., d’Agostino, M.V., Madeo, A.: Identification of scale-independent material parameters in the relaxed micromorphic model through model-adapted first order homogenization. *Journal of Elasticity* **139**(2), 269–298 (2020)
- [5] Neff, P., Ghiba, I.D., Madeo, A., Placidi, L., Rosi, G.: A unifying perspective: the relaxed linear micromorphic continuum. *Continuum Mechanics and Thermodynamics* **26**(5), 639–681 (2014)
- [6] Schröder, J., Sarhil, M., Scheunemann, L., Neff, P.: Lagrange and $H(\text{curl}, \mathcal{B})$ based finite element formulations for the relaxed micromorphic model. *Computational Mechanics* (2022)
- [7] Sky, A., Muench, I., Neff, P.: On $[H^1]^{3 \times 3}$, $[H(\text{curl})]^3$ and $H(\text{symCurl})$ finite elements for matrix-valued Curl problems. *Journal of Engineering Mathematics* **136**(1), 5 (2022)
- [8] Sky, A., Neunteufel, M., Muench, I., Schöberl, J., Neff, P.: Primal and mixed finite element formulations for the relaxed micromorphic model. *Computer Methods in Applied Mechanics and Engineering* **399**, 115298 (2022)

- [9] Sky, A., Neunteufel, M., Münch, I., Schöberl, J., Neff, P.: A hybrid $H^1 \times H(\text{curl})$ finite element formulation for a relaxed micromorphic continuum model of antiplane shear. *Computational Mechanics* **68**(1), 1–24 (2021)
- [10] Zaglmayr, S.: High order finite element methods for electromagnetic field computation. Ph.D. thesis, Johannes Kepler Universität Linz (2006). URL <https://www.numerik.math.tugraz.at/~zaglmayr/pub/szthesis.pdf>